

# Future Extension Of The UK Summer And Its Impact On Autumn Precipitation

Daniel F. Cotterill (✉ [daniel.cotterill@metoffice.gov.uk](mailto:daniel.cotterill@metoffice.gov.uk))

Met Office <https://orcid.org/0000-0003-1509-7506>

James O. Pope

Met Office

Peter A. Stott

Met Office

---

## Research Article

**Keywords:** Anthropogenic Climate Change, Atmospheric Circulation, Precipitation, Drought, Attribution.

**Posted Date:** March 11th, 2022

**DOI:** <https://doi.org/10.21203/rs.3.rs-1427756/v1>

**License:**  This work is licensed under a Creative Commons Attribution 4.0 International License. [Read Full License](#)

---

# Abstract

Research into weather circulation changes over the UK for future climate has mainly focused on changes in the Summer and Winter seasons, with less analysis on seasonality and the transition seasons. Using the 30 Met Office weather patterns we examine the influence of climate change on seasonality through atmospheric circulation using a number of climate models. Changes in seasonality are important as they can have large impacts on many sectors including agriculture, energy and tourism. This paper finds a noticeable increase in Autumn over the UK in the frequency of drier summer-type regimes and a decrease in stormy winter types that emerge as early as the 2020s. The change in circulation signal once isolated from the overall signal is responsible for a 4-12% decrease in Autumn mean rainfall on average for England by the end of this century (where the values in the range are dependent on the emissions scenario). This change is projected over English regions that are already experiencing water stress, and with predictions of drier summers over the UK in future, this could further increase drought risk. The change in circulation in Autumn also moderates the large increase in the number of large-scale extreme daily rainfall events over the same regions predicted due to climate change. While climate models replicate the frequency of the 30 weather patterns well for all seasons, large differences remain between the strength of circulation signal changes simulated by models even though the general trend is in agreement.

## 1. Introduction

In the UK both precipitation and temperature extremes are projected to increase significantly with anthropogenic climate change (Hanlon et al., 2021; Christidis et al., 2020; Cotterill et al., 2021; Kendon et al., 2014). However, less attention has been given to how much atmospheric circulation changes are contributing to these long-term projected changes in addition to the thermodynamic changes, particularly within the transition seasons. Atmospheric circulation impacts the probability of extreme events over Europe significantly, with many attribution studies of extreme events examining changes in probability of the event for given atmospheric conditions (Christidis et al., 2015; Schaller et al., 2016).

Atmospheric circulation and weather types have been examined for a long time for the UK including the seven Lamb weather types (Lamb, 1972) which have been developed and used further (Jenkinson, 1977) (Jones et al., 1993). Since then, there has been a shift to creating circulation types using k-means clustering. Fereday et al., 2008 created 10 weather patterns for each season using mean sea level pressure (psl), Ferranti et al., 2015 created 4 weather patterns using geopotential height and most recently Neal et al., 2016 created the 30 weather patterns which are used at the Met Office as a forecasting tool. The 30 weather patterns cover the UK and the north-west European domain. The benefit of using the 30 weather patterns is that they don't only provide information on broadscale circulation, but variations within it, including seasonality (Neal et al., 2016). Studies have started using the 30 weather patterns for research into future and current circulation changes and their relation to climate hazards using the UK Climate Projections (UKCP). Pope et al., 2021 finds that circulation changes will lead to more dry summers and more westerly and cyclonic conditions in the winter and Kendon et al., 2020 examine which patterns are most likely to lead to record breaking warm winter events such as February of 2019 in the UK.

There is still a lot of uncertainty on atmospheric changes over the European region, especially due to their link to the Atlantic Meridional Overturning Circulation (AMOC). There are large differences in the projected weakening of the AMOC in models, the strength thereof would impact the changes in European climate through the uncertainty of heat transport (Haarsma et al., 2015). Rahmstorf et al., 2015 provide evidence of the slowdown of AMOC in the 20th

century leading to a cooling of a region in the North Atlantic, with this subpolar cooling much weaker in the CMIP5 models than seen in the observations.

Some studies are already finding differences in atmospheric circulation over Northern Europe. Schaller et al., 2016 using current and counterfactual climate conditions find that an increase in low-pressure systems northwest of the UK in winter and change in zonal flows is already occurring because of anthropogenic influence. Another study finds that changes in atmospheric conditions using clustering are already being seen in the observations with the summer extending into early autumn and late spring since 1948 (Vrac et al., 2013). Seasonal changes are likely to have a big impact on the Agriculture, Energy and Tourism sectors (Vrac et al., 2013). An analysis using the UKCP projections finds that the summer dry season is longer in the future with less soil moisture in the summer and autumn (Pirret et al., 2020). The UK has already experienced impacts from droughts, a dry period from 2016–2019 caused a number of impacts including agriculture, wildfires and freshwater ecosystems, especially in the South-East of England (Turner et al., 2021).

This paper will look at whether circulation changes through weather patterns may be contributing to these changes and by how much. This work will address three main scientific questions. Firstly, using attribution runs, has anthropogenic influence noticeably changed the frequency of weather patterns over the UK already? Secondly, are there future changes in seasonality due to circulation, and if so, how does this change vary between emissions scenarios and models? Finally, what is the impact of these changes in seasonality on mean and extreme rainfall for the UK? This last question will be addressed by isolating the atmospheric circulation signal from the overall signal.

## **2. Data And Methods**

### **2.1 Data**

#### **2.1.1 ERA5 Weather Patterns**

To evaluate how well each of the models capture the frequency of daily weather patterns, the ERA5 reanalysis data from the European Centre for Medium Range Weather Forecasting (ECMWF) covering the period 1979–2010 was used. This data with a horizontal resolution of 31km and 137 vertical levels up to 0.01 hPa uses Observations, Models and a 4D-Var data assimilation scheme to produce high resolution global reanalyses (Hersbach et al. 2020). The weather patterns were assigned to the ERA5 daily mean sea level pressure data using the method described in Neal et al (2016).

#### **2.1.2 HadGEM3-A**

The HadGEM3-A is a global atmospheric climate model created in the UK Met Office Hadley Centre with a horizontal resolution of 60 km at the mid-latitudes. This contains 15 ensemble members for each ALL forcings (historical) ensemble and NAT forcings (hist-nat) ensemble from 1960 to 2013 and larger sets of ensembles beyond that until present. The hist-nat runs contain anthropogenic forcings held at 1850 levels with changes in Natural forcings only, and historical represents all forcings as they actually evolved (Vautard et al., 2018). The boundary conditions for both ALL and NAT simulations use observed sea surface temperatures and sea ice, which are adjusted in the NAT ensemble by having an estimate of the changes due to human induced climate change removed. More information can be found in Christidis et al., 2013 and Ciavarella et al., 2018.

#### **2.1.3 UKCP PPE**

The UK Climate Projections contains 28 global ensemble-members (15 Hadley Centre and 13 CMIP5 models) from 1899–2099 for different emissions emission scenarios ranges (Lowe et al., 2019). For this work we use the 15 Hadley Centre perturbed parameter ensemble (PPE) members. The 15 PPE members are based on the HadGEM model at GC 3.05 configuration, and the construction of the PPE is discussed in Sexton et al. (2021) and Yamazaki et al. (2021). A summary of the simulations is available in Pope et al. (2021). This paper uses daily precipitation and pressure at sea level (psl) data for both the lowest and highest emission scenario runs, Representative Concentration Pathways (RCP) RCP 2.6 and RCP 8.5 respectively. These scenarios were created to account for a range of outcomes, including future greenhouse gas emissions and mitigation, economic factors and population changes (Lowe et al., 2018). The UKCP PPE weather regime data for RCP 2.6 and RCP 8.5 between 1899–2099 was the same data created and used in Pope et al 2021 from daily psl data.

## **2.1.4 HadUK- Grid Observations**

The HadUK-Grid gridded observations dataset is used to evaluate climate model data for regional precipitation in the UK. This dataset produced by the Met Office Hadley Centre is based on land surface observations and is available both at a number of gridded resolutions and a regional level for 16 administrative regions (Hollis et al., 2019). This paper uses the regional daily precipitation dataset over the time period 1970–2000.

## **2.1.5 CMIP6 Models**

The following two CMIP6 models were chosen because they were the only ones that had four or more ensemble members with a high future emissions scenario and had a resolution of 100 km or less.

MRI-ESM2-0 (CMIP6): Data from CMIP6 from the Earth System Model MRI-ESM2-0, created by the Meteorological Research Institute in Japan, with a horizontal resolution of 100 km (Yukimoto et al., 2019). The data used for this work came from two of the experiments, hist-nat (containing only changes in Natural forcings) and a shared socio-economic pathway SSP3-7.0 (a future medium/high emissions scenario, see Meinshausen et al., 2020 for more details).

HadGEM3-GC31-MM (CMIP6): Data from CMIP6 from the Global Climate Model HadGEM3-GC31 created by the UK Met Office Hadley Centre with a horizontal resolution of 60 km at the mid-latitudes (Ridley et al., 2019). The data used from this work came from two experiments, historical and a shared socio-economic pathway SSP5-8.5 (a future high emissions scenario, see Meinshausen et al., 2020 for more details).

## **2.1.6 The Met Office 30 UK Weather Patterns**

The Met Office 30 Weather Patterns (Neal et al., 2016) are a set of patterns aiming to cover the large range of circulation types over the UK and the European Domain (the North Atlantic-European (NAE) Domain). These patterns verified by UK Meteorologists were created using the EMULATE (European and North Atlantic daily to multidecadal climate variability- Ansell et al., 2006) sea level pressure reanalysis data from 1850–2003 in combination with a k-means clustering algorithm (Philipp et al. 2007), over the NAE domain (30°W–20°E; 35°–70°N). The lower numbers have lower psl anomalies, which occur more in the summer and will be referred to as summer-types and the high numbered weather patterns which have very high psl anomalies occurring more in the winter, will be referred to as winter-types (Neal et al. 2016).

## **2.2 Methods**

### **2.2.1 Allocating weather patterns to climate model data**

To assign weather pattern values to daily climate model data, the methodology used in (Neal et al 2016) was applied. Daily weather pattern numbers are assigned to climate model data by calculating the daily psl anomalies for the model data and comparing them to each of the 30 weather patterns. This is done through the area-weighted sum of squares difference (referred to as the distance) calculated at each grid point, with the pattern with the smallest distance value being assigned to that day in the model. For the distance calculation, the model psl anomalies were re-gridded to the same resolution as the 30 weather patterns created using the EMULATE data.

The climate model data psl anomalies are created by taking a climatological average over a baseline period for each day of the year and comparing that to the respective day of the year for the daily climate model data. The climatological average was created for each ensemble member individually, with the choice of baseline period the same for each ensemble member. This was applied to the CMIP6 models used and the HadGEM3-A model runs, with the UKCP model daily weather data already available. All three models used the hist-nat/historic runs from 1960/70-2000/10 as the baseline period, with the exception of the HadGEM3-GC31-MM from CMIP6. The details of the choice of baseline period for each model can be found in Supplementary Table 1. The UKCP weather regime data used was created in the same way but had a longer baseline period of 1900–1999 using historic runs (Pope et al., 2021). The climatologic average over the baseline period for a given ensemble member was used for all time slices and emissions scenarios for that ensemble member.

## 2.2.2 Measuring confidence in the results

To examine the strength of changes between two different time-slices or emission scenarios in the frequency of weather patterns for a given weather pattern,  $wp$  we use a bootstrapping with replacement method. Weather patterns are compared individually instead of all 30 at once, because consecutive regimes are not directly related to each other and are unique.

The following steps are used to examine whether weather pattern changes between two time-slices named  $ts1$  and  $ts2$  for a specific weather pattern  $wp$  in a specific season is significant:

- Firstly, for each year of data in the time-slice produce count values for the number of days with pattern  $wp$  over the season of interest. For a time-slice of length  $n$  years and  $m$  number of ensemble members there are  $n \times m$  season-year count values.
- For each time-slice these season-year count values are bootstrapped with replacement 10 000 times
- After every bootstrap the count values are summed across all years in the time-slice giving totals counts for time-slices  $ts1$  and  $ts2$ ,  $count_{ts1}$  and  $count_{ts2}$  respectively.
- The change for a given pattern is significant if  $count_{ts1} > count_{ts2}$  for 97.5% or  $count_{ts1} < count_{ts2}$  for 2.5% of the bootstrapped values for that pattern. This is a measure of how much the ranges overlap which we will refer to as a significant range difference.

## 2.2.3 Isolating the circulation signal using weather pattern frequencies

To isolate the climate signal for circulation, we use both the changes in daily frequencies of the 30 weather patterns and climatology profiles of each regime for the chosen variable. The method follows as such for examining the impact of a circulation signal change in variable  $X$ , which for this example is extreme precipitation days (99.5th percentile) for the season of interest.

Climatology Profile: Firstly, a baseline period for the climatology was chosen, which is the UKCP Global data between 1900–1950. This is because there are a large number of ensemble members (15) over a long time period and hence a sufficient number of extreme events to produce profiles for each pattern. The time period also occurs far in the past where signals of anthropogenic climate change have not emerged significantly yet. Using daily rainfall data associated with each pattern using the UKCP data, the probability of an extreme rainfall day ( $p_{wp}$ ) on any day given its weather pattern ( $wp$ ), is calculated. The definition of an extreme rainfall day for a particular season, is a day where the daily precip exceeds the 99.5th percentile over the baseline period (1900–1950). This was also carried out for mean rainfall, where in the climatology profile instead of it being a probability of an extreme rainfall day- it was the mean rainfall for a day of a given pattern.

Frequency profile: For each of the models examined the pattern frequency is calculated for the two time-slices to be compared individually. In each case a historical/hist-nat time-slice ( $ts_{past}$ ) is compared to a future time time-slice ( $ts_{future}$ ) under a given emissions scenario over the following time periods:

- (i) Historical Period/Hist-nat period- January 1970 to December 1999
- (ii) Future Period (RCP 2.6/8.5 and SSP370/585)- January 2071 to November 2099

Based on the weather pattern frequencies in the two time-slices being compared, the expected number of days for each weather pattern  $wp$  ( $number\_days_{wp}$ ) over a 20-year period for both  $ts_{past}$  and  $ts_{future}$  for the chosen season is calculated. Then using  $p_{wp}$  from the climatology profile and  $number\_days_{wp}$ , the projected percentage increase in the number of extreme days between time slices  $ts_{past}$  and  $ts_{future}$  based off the change in frequency of weather patterns alone can be calculated using formulas 1 and 2.

$$Expectedextremeraingdays_{ts} = \sum_{wp=1}^{30} EquationNumber\_days_{wp} * probextremeday_{wp}$$

1

$$\Delta changeinEquationNumberofextremedays(\%) = \left( \frac{Expectedextremeraingdays_{ts\_future}}{Expectedextremeraingdays_{ts\_past}} - 1 \right) * 100\%$$

2

To produce the same calculation, but for mean precipitation instead of extreme precipitation, formulas 3 and 4 are used where  $mean\_precipitation_{wp}$  is the mean daily precipitation for weather pattern  $wp$ . The uncertainty in the results from formulas (1–4) for the circulation signal is estimated using the model range. These results give an estimate of the change in the variable of interest due to the isolated Atmospheric Circulation Signal (ACS).

$$Expected20yerrainfall_{ts} = \sum_{wp=1}^{30} EquationNumber\_days_{wp} * mean\_precipitation_{wp}$$

3

$$\Delta changeinmeanrainfall(\%) = \left( \frac{Expected20yerrainfall_{ts\_future}}{Expected20yerrainfall_{ts\_past}} - 1 \right) * 100\%$$

4

To show these changes from the ACS in context, the overall signal change is also calculated. The overall signal change in these variables between a past and future time-slice for a given emissions scenario is calculated separately using data from the UKCP Global in each time-slice. The uncertainty on the overall signal is estimated using bootstrapping with replacement for the daily rainfall data over the region. After bootstrapping the daily precipitation data 10 000 times, the 99.5th percentile of daily rainfall and mean yearly rainfall for the chosen season are calculated 10 000 times. The 95% confidence intervals calculated for each are then compared between time-slices to produce upper and lower estimates of the overall change in each variable between the time-slices.

## 3 Model Evaluation

### 3.1 Attribution runs

The model used for the attribution of weather patterns, HadGEM3-A is validated for weather pattern frequencies over the time period 1979–2010, using the ERA5 reanalysis data. The 15 ensemble members from the ALL forcings runs of the HadGEM3-A are shown as boxplots in Fig. 1, where strong agreement can be seen for all seasons between the HadGEM3-A model and ERA5. The ERA5 reanalyses fall within the model range for 29/26/26/28 out of 30 regimes for Winter/Spring/Summer/Autumn (djf/mam/jja/son) respectively. The few regimes where observation lie outside the model range for each season are only slightly outside the ensemble range.

### 3.2 Model validation of UKCP and CMIP6 model data for weather patterns

Pope et al., 2021 evaluates both the annual frequency of the 30 weather patterns and persistence within the UKCP Global climate projections finding that there is good agreement between the UKCP Global members and ERA5. A further evaluation of seasonal frequencies for UKCP Global 15 PPE members used in this paper, shows the strong agreement between the model and ERA5, with the ERA5 data falling within the UCKP 15 PPE models range for 21/29/25/26 out of the 30 patterns for djf/mam/jja/son respectively. The two CMIP6 models chosen HadGEM3-GC31-MM (4 ensemble members) and the MRI-ESM2-0 (5 ensemble members) when combined and compared against the ERA5 data also show relatively strong agreement. The ERA5 data falls within the CMIP6 models range for 15/23/26/27 out of the 30 patterns for djf/mam/jja/son respectively. The CMIP6 models show some deviations from the observations in winter, compared to the other seasons, similar to the UKCP Global 15 PPE. However, for this evaluation only 9 model ensemble members were used for CMIP6, and these models are not used to analyse winter weather pattern changes in this paper.

### 3.3 Model validation of UKCP Global for rainfall

The UKCP Global 15 PPE between 1900–1950 is used as the baseline for the rainfall climatology for each of the 30 weather patterns. The model validation is chosen over a later period for the model, where the quality of observations is improved (1970–2000).

The UKCP Global projections show regional variation in its ability to capture UK rainfall in Autumn (Fig. 2). The model agrees more with the observations for flatter regions of the UK for mean and extreme rainfall (99th percentile). Therefore, for the climatological examination of the changes in UK rainfall in Autumn, this work focusses on three distinctly located regions where the observations for both mean yearly rainfall and the 99th percentile of daily rainfall in Autumn fall within the model ensemble range. These are chosen as South East England, the West Midlands and Yorkshire and Humber with the model data coverage of that region shown in Fig. 6.

## 4 Results

### 4.1 Attribution of weather patterns

To assess whether there has been an anthropogenic influence on the patterns seen over the UK, seasonal frequencies of weather patterns are compared for HadGEM3-A, which contains both 15 members ensembles with Natural Forcings only and with All Forcings (Fig. 3). The figure shows that for all seasons between 1980-2010 there are very few noticeable differences in pattern frequencies between ALL and NAT with there being no significant range differences for 28/26/23/25 of the 30 weather patterns for djf/mam/jja/son respectively. The same analysis was carried out for MRI-ESM2-0 for the 5 NAT and 5 ALL ensemble members between 1980-2010. This showed a few extra noticeable differences with no significant range differences for 22/27/28/19 out of the 30 patterns for djf/mam/jja/son respectively. The patterns out of the 30 that showed significant range differences were compared for both models and there was very little agreement between the two models on these weather pattern changes with no overarching trends (Supplementary Table 2). The only weather patterns that showed the same change in both models were pattern 20 (increasing in frequency in SON), pattern 5 (decreasing in frequency in SON), and pattern 29 (increasing in frequency in MAM). Overall, based on these models, no clear signal has appeared suggesting that anthropogenic climate change has not influenced the frequency of weather patterns significantly before 2010.

### 4.2 Future climate signal in weather regimes

To assess the influence of anthropogenic climate change on weather patterns in the future, the UKCP Global is examined for a past period (1960-2010), as well as a future period (2071-2100) for both a low (RCP 2.6) and high (RCP 8.5) emissions scenario. Given very few significant range differences were found between ALL and NAT forcings from 1980-2010, the historic period is used as a baseline for weather pattern frequencies when looking at the influence of anthropogenic climate change on the ACS.

The results show that there are significant range differences for the majority of the 30 weather patterns within all seasons between UKCP Global historic and future RCP 8.5. Figure 4 shows the differences for Autumn with the boxplots for future RCP 2.6 falling between the past and future RCP 8.5 time slices, indicating that anthropogenic influence is behind these changes in weather pattern frequencies. The main pattern seen in this figure for Autumn, is that there are significant increases in the lowest numbered patterns (summer-types) and a decrease in the highest numbered patterns (winter-types). This is also seen for the season of Summer, but not Winter or Spring in the UKCP projections (Supp. Fig. 4-6). These differences seen between the lowest and highest emission scenarios in the future are much greater than the differences seen between the past and the future low emissions scenario.

The CMIP6 models also show the same trends in Autumn but to a lesser extent, with a large increase in the lower numbered summer-type weather patterns and a decrease in the higher-numbered winter-type ones (Fig. 5). This change can also be seen in the Summer in MRI-ESM2-0 and HadGEM3-GC31 (Supplementary Table 3), however such a trend is not seen in Spring or Winter. This extension of the summer seen in the models could have big impacts on a number of weather variables including rainfall- which is examined in detail in the next section. It is also important to note that these changes have not appeared to occur in weather patterns seen when comparing ALL and NAT forcings before 2010 in the attribution section.

To examine when this signal emerges, the combined frequency of the predominantly summer type patterns (1-6) is plotted against the combined frequency of the predominantly winter type patterns (25-30) for the lowest and highest emissions scenarios for UKCP Global RCP 2.6 and RCP 8.5 respectively (Fig. 6). This shows that the signal could emerge as early as 2025 under these scenarios with the two emissions scenarios deviating to outside the 1900-2000

range from around 2035 onwards. By Autumn 2095 the frequency of winter-type patterns in SON could decrease by over a third under the highest emissions scenarios and summer-types increasing by a quarter. Under low emissions this change in seasonality in Autumn is much reduced as can be seen in figure 6.

### 4.3 Impacts of weather pattern changes on UK rainfall

To investigate whether the increase in summer-type patterns impacts rainfall, the ACS is isolated and compared to the overall change. The main focus of this analysis is for Autumn, given the strong signal seen in section 4.2. To assess the relative impact of the ACS against the overall signal, the method used in section 2.3 is applied for a past time period (1971-2000) and the future time period (2071-2100) under different emissions scenarios for Autumn, using the three regions chosen (Fig. 7). The climatology profile for each weather pattern for both the probability of an extreme rainfall day in Autumn (SON) (a day exceeding 99.5<sup>th</sup> percentile) and mean SON daily rainfall is calculated from the UKCP Global dataset over a baseline period running from 1900-1950.

Future circulation changes in the models when isolated show a 9-12% decrease in mean rainfall in SON from 1985 to 2085 over the three English regions (Table 1). The signal of this change is true for all 3 models examined under high emissions scenarios, with the strongest signals seen in the UKCP Global RCP 8.5 and HadGEM3-GC31 ssp585, with the MRI-ESM2-0 ssp370 showing a weaker ACS. The overall signal for Autumn mean rainfall, a decrease of 9-11% using the UKCP Global RCP 8.5 simulations is almost identical to the ACS, a decrease of 9-12%. This suggests that the overall mean rainfall signal leading to drier Autumns in the future is primarily driven by atmospheric circulation changes. Future ACS changes in the models when isolated also shows a 21-23% decrease in extreme daily rainfall events in Autumn (Table 1). The overall signal over the same time interval, however, shows a 71-103 % increase in extreme rainfall days in SON using the UKCP Global RCP 8.5 simulations. This would likely be even higher if it wasn't moderated by the 21-23% decrease due to the ACS.

Table 1: The change in rainfall indices between 1985 and 2085 for both the ACS and overall signal in Autumn. The two indices are the percentage change in mean precipitation ( $\Delta$  mean pr) and the percentage change in the number of extreme rainfall days exceeding the 99.5<sup>th</sup> percentile ( $\Delta$  99.5<sup>th</sup> percentile daily pr). The uncertainty in the ACS comes from the model range (MR) as multiple models are examined, and for the overall signal using the UKCP Global 15 ensemble members, the 95% confidence intervals (CI) are used.

Administrative Region	Circulation Only ( $\Delta$ mean pr) %	Overall Signal ( $\Delta$ mean pr) %	Circulation Only ( $\Delta$ 99.5th percentile daily pr) %	Overall Signal ( $\Delta$ 99.5th percentile daily pr) %
South East England	-12 (MR: -6--16)	-11 (CI: -15--7)	-21 (MR: -28--10)	103 (CI: 61-158)
West Midlands	-9 (MR: -4--13)	-11 (CI: -15--8)	-22 (MR: -28--11)	71 (CI: 34-119)
Yorkshire and Humber	-9 (MR: -4--12)	-9 (CI: -13--6)	-23 (MR: -30--12)	75 (CI:38-125)

There are also big differences for rainfall indices between emission scenarios RCP 2.6 and RCP 8.5 for UKCP Global, both for the ACS and overall signal (Table 2). Overall, under a low emissions scenario the increase in Autumn extreme rainfall days is around 21-47 % depending on the region, compared to 71-103 % under the highest emissions scenario at the end of this century. The difference is even more pronounced for mean rainfall where there is only a 5% decrease in mean rainfall compared to a 10% decrease, when comparing RCP 2.6 and RCP 8.5 respectively. The ACS is also significantly reduced for both indices under a lower emissions scenario, with the signal between 2-3 times greater for the higher emissions scenario.

Table 2: The change in rainfall indices between 1985 and 2085 for both the ACS and the overall signal for different UKCP Global emissions scenarios. The two indices are the percentage change in mean precipitation ( $\Delta$  mean pr) and the percentage change in the number of extreme rainfall days exceeding the 99.5<sup>th</sup> percentile ( $\Delta$  99.5<sup>th</sup> percentile daily pr).

Administrative Region	Circulation Only ( $\Delta$ mean pr) %		Overall Signal ( $\Delta$ mean pr) %		Circulation Only ( $\Delta$ 99.5th percentile daily pr) %		Overall Signal ( $\Delta$ 99.5th percentile daily pr) %	
	RCP 2.6	RCP 8.5	RCP 2.6	RCP 8.5	RCP 2.6	RCP 8.5	RCP 2.6	RCP 8.5
South East England	-5	-14	-4	-11	-9	-25	47	103
West Midlands	-4	-10	-6	-11	-9	-26	21	71
Yorkshire and Humber	-4	-11	-4	-9	-10	-28	30	75

## 5 Discussion And Conclusions

In this paper we have found a climate circulation signal showing a predicted increase in the frequency of predominantly summer-type and a decrease in predominantly winter type weather patterns in both Autumn and Summer over the UK. This climate signal could emerge as early as the 2020s based on the UKCP projections. The estimated impact of what this signal means for Autumn mean and extreme rainfall is examined for multiple English regions. We find that these changes in the frequency of weather patterns could result in up to a 5–14% decrease in mean Autumn rainfall for English regions by 2085, dependent on the emissions scenario (RCP 2.6 – RCP 8.5). The overall mean reduction of rainfall in Autumn seen in the UKCP Global is of almost the same magnitude as the reduction in rainfall due to changes in the frequency of weather patterns, suggesting that circulation is playing a dominant role in these changes. This combined with drier summers predicted by the UKCP projections (Lowe et al., 2019) has big implications for future risks of drought over the UK, especially given parts of England have only recently experienced some of the impacts from drought.

There are however both strong differences between models and emission scenarios for the magnitude of this change. The decrease in Autumn rainfall due to circulation in the UKCP Global is three times smaller for the lowest emissions scenario RCP 2.6 than the highest emissions scenario RCP 8.5. Furthermore, this circulation climate signal seen in Autumn producing drier weather is around 3 times smaller in the MRI-ESM2-0 compared to the other two models, with the difference between the models being the main uncertainty in these results.

Despite drier Autumns, there is a large increase in the number of extreme rainfall days in SON of up to 47–103% (RCP 2.6- RCP 8.5) by the end of this century. We do find that changes in circulation for Autumn moderate this increase and the circulation signal when isolated from the overall signal acts to reduce the number of extreme rainfall days over parts of England by 21–23%. This could explain why we see a larger increase in winter daily rainfall extremes than in Autumn by the end of this century in the UKCP projections (Cotterill et al., 2021).

Despite these future changes, no obvious detectable changes have been found when comparing the NAT forcings runs to the ALL forcings runs for any of the seasons before 2010. Even for those of the 30 regimes that show small differences between ALL and NAT for models, there is very little agreement between the two models examined HadGEM3-A and MRI-ESM2-0. One could argue that a greater number of simulations than the 20 each from ALL/NAT are required to examine changes for weak signals, but these results suggest that this Extension of Summer is not visible before 2010. The UKCP Global suggests that under both the low and high emissions scenarios, this Autumn circulation signal with more summer-type and less winter-type regimes will emerge in the next decade or so

(Fig. 6). The magnitude of this change by the end of this century, however, is heavily dependent on the emissions scenario.

Despite the detail of the 30 weather regimes the climate models used had strong agreement with the Observations for all seasons, especially the HadGEM3-A. This may be expected as the model uses SST and Arctic Sea Ice as boundary conditions, therefore constraining it more to the global patterns over the time period examined. However, there are limitations to this method at only looking at the daily frequencies of weather patterns. Firstly, that for days that show a transition between two patterns could end up showing the average of the two psl patterns which could be a completely different pattern to those two. Secondly, the weather patterns based on observations from 1850–2010, may evolve and be less suited to future patterns and associated impacts. Multidecadal variability may have also impacted the results when comparing the two time slices. But given the strength of this atmospheric climate signal, found in this work in Autumn being both very strong and seen across all models, there can be confidence in the results.

This paper mainly focusses on the impacts of the circulation signal on rainfall for Autumn, but there are a number of other possible impacts as a result of this climate signal including heat stress and impacts for agriculture. This could be a good area for future research with the number of sectors and industries that these long-term changes could impact, with large differences seen between the lowest and highest emissions scenarios. The impacts of these could also be examined using the UKCP18 2.2km convective permitting model, to look at the regional impacts of these long-term changes.

## 6 Statements And Declarations

### 6.1 Acknowledgements

D. Cotterill thanks the UKRI Strategic Priorities Fund for funding this research at the UK Met Office as part of the UK Climate Resilience Programme. J.O. Pope was supported by the Met Office Climate Service for Food, Farming and Natural Environment, funded by the Department for Environment, Food and Rural Affairs (Defra) Climate Service. P. A. Stott was supported by the Hadley Centre Climate Programme (HCCP) and also the UK Climate Resilience Programme (UKCR).

### 6.2 Data

The data from the UKCP Global model used in this study is available from the Centre for Environmental Data Analysis (<http://data.ceda.ac.uk/badc/ukcp18/data>). More information on this dataset can be found under (Lowe et al., 2018). For the UKCP Global data set, model numbers 1-15 represent the UKCP Global PPE and numbers 16–28 the UKCP Global CMIP5-13. The weather pattern data for the UKCP Global ensemble is available from the Centre for Environmental Data Analysis using the link above. The Weather Pattern data created in this work for other models, described in detail in Supplementary Table 1 is available on reasonable request, as is the UKCP Global PPE-15 weather pattern data for RCP 2.6.

### 6.3 Competing Interests

The authors have no known competing financial interests or personal relationships to disclose that could have appeared to influence this paper.

## References

1. Ansell TJ, Jones PD, Allan RJ et al (2006) Daily mean sea level pressure reconstructions for the European–North Atlantic region for the period 1850–2003. *J Clim* 19:2717–2742. <https://doi.org/10.1175/JCLI3775.1>
2. Christidis, N., Stott, P. A., Scaife, A. A., Arribas, A., Jones, G. S., Copey, D., Knight, J. R., & Tennant, W. J. (2013). A New HadGEM3-A-Based System for Attribution of Weather- and Climate-Related Extreme Events, *Journal of Climate*, 26(9), 2756-2783. Retrieved Feb 17, 2022, from <https://journals.ametsoc.org/view/journals/clim/26/9/jcli-d-12-00169.1.xml>
3. Christidis, N., Stott, P.A., 2015. Extreme Rainfall in the United Kingdom During Winter 2013/14: The Role of Atmospheric Circulation and Climate Change [in “Explaining Extremes of 2014 from a Climate Perspective”]. *Bull. Amer. Meteor. Soc.*, 96 (12), S46-S50.
4. Christidis, N., McCarthy, M. & Stott, P.A. The increasing likelihood of temperatures above 30 to 40 °C in the United Kingdom. *Nat Commun* 11, 3093 (2020). <https://doi.org/10.1038/s41467-020-16834-0>
5. Ciavarella, A., Christidis, N., Andrews, M., Groenendijk, M., Rostron, J., Elkington, M., Burke, C., Lott, F.C., Stott P.A., 2018. Upgrade of the HadGEM3-A based attribution system to high resolution and a new validation framework for probabilistic event attribution. *Weather Clim. Extrem.*, 20, pp. 9-32, <https://doi.org/10.1016/j.wace.2018.03.003>.
6. Cotterill, D., Stott, P., Christidis, N. and Kendon, E. (2021) Increase in the frequency of extreme daily precipitation in the United Kingdom in autumn. *Weather and Climate Extremes*.
7. Fereday DR, Knight JR, Scaife AA, Folland CK, Philipp A. 2008. Cluster analysis of North Atlantic–European circulation types and links with tropical Pacific sea surface temperatures. *J. Clim.* 21: 3687– 3703.
8. Ferranti L, Corti S, Janousek M. 2015. Flow-dependent verification of the ECMWF ensemble over the Euro-Atlantic sector. *Q. J. R. Meteorol. Soc.* 141: 916– 924, DOI: 10.1002/qj.2411.
9. Hanlon, H.M., Bernie, D., Carigi, G. et al. Future changes to high impact weather in the UK. *Climatic Change* 166, 50 (2021). <https://doi.org/10.1007/s10584-021-03100-5>
10. Hersbach H, Bell B, Berrosfprd P et al (2020) The ERA5 global reanalysis. *Q J R Meteorol Soc* 146:1999-2049. <https://doi.org/10.1002/qj.3803>
11. Hollis, D., McCarthy, M., Kendon, M., Legg, T., Simpson, I., 2019. HadUK-Grid—A new UK dataset of gridded climate observations. *Geosci Data J.*; 6: 151– 159. <https://doi.org/10.1002/gdj3.78>
12. Jenkinson AF, Collison FP. 1977. An Initial Climatology of Gales over the North Sea. *Synoptic Climatology Branch Memorandum No. 62*. Meteorological Office: Bracknell.
13. Jones PD, Harpham C, Briffa KR. 2013. Lamb weather types derived from reanalysis products. *Int. J. Climatol.* 33: 1129– 1139.
14. Kendon, E., Roberts, N., Fowler, H. et al. Heavier summer downpours with climate change revealed by weather forecast resolution model. *Nature Clim Change* 4, 570–576 (2014). <https://doi.org/10.1038/nclimate2258>
15. Kendon, M., Sexton, D. and McCarthy, M. (2020), A temperature of 20°C in the UK winter: a sign of the future?. *Weather*, 75: 318-324. <https://doi.org/10.1002/wea.3811>
16. Lamb HH (1972) British Isles weather types and a register of the daily sequence of circulation patterns 516 1861–1971. *Geophys. Mem.* 116: 85
17. Lowe, J.A., Bernie, D., Bett, P.E., Bricheno, L.M., Brown, S.C., Calvert, D., Clark, R., Karen, Eagle, Edwards, T.L., Fosser, G., Maisey, P., McInnes, R.N., Mcsweeney, C., Yamazaki, K., & Belcher, S., 2019. UKCP18 Science Overview Report November 2018 (Updated March 2019). <https://www.metoffice.gov.uk/pub/data/weather/uk/ukcp18/science-reports/UKCP18-Overview-report.pdf>

18. Meinshausen, M., Nicholls, Z. R. J., Lewis, J., Gidden, M. J., Vogel, E., Freund, M., Beyerle, U., Gessner, C., Nauels, A., Bauer, N., Canadell, J. G., Daniel, J. S., John, A., Krummel, P. B., Luderer, G., Meinshausen, N., Montzka, S. A., Rayner, P. J., Reimann, S., Smith, S. J., van den Berg, M., Velders, G. J. M., Vollmer, M. K., and Wang, R. H. J.: The shared socio-economic pathway (SSP) greenhouse gas concentrations and their extensions to 2500, *Geosci. Model Dev.*, 13, 3571–3605, <https://doi.org/10.5194/gmd-13-3571-2020>, 2020.
19. Neal R, Fereday D, Crocket R, Comer R (2016) A flexible approach to defining weather patterns and their application in weather forecasting over Europe. *Meteorol Apps* 23:389-400 <https://doi.org/10.1002/met.1563>
20. Pirret, J.S.R., Fung, F., Lowe, J.A., McInnes, R.N., Mitchell, J.F.B. and Murphy, J.M. (2020). UKCP Factsheet: Soil Moisture. Met Office.
21. Philipp A, Jacobeit J, Della-Marta PM, Wanner H, Fereday DR, Jones PD, et al. 2007. Long-term variability of daily North Atlantic–European pressure patterns since 1850 classified by simulated annealing clustering. *J. Clim.* **20**: 4065–4095.
22. Pope, J.O., Brown, K., Fung, F., Hanlon, H.M., Neal, R., Palin., E.J. & Reid, A. (2021) Investigation of Future Climate Change Over the British Isles using Weather Patterns. *Climate Dynamics*
23. Rahmstorf, S., Box, J., Feulner, G. et al. Exceptional twentieth-century slowdown in Atlantic Ocean overturning circulation. *Nature Clim Change* 5, 475–480 (2015). <https://doi.org/10.1038/nclimate2554>
24. Reindert J Haarsma et al 2015 *Environ. Res. Lett.* 10 094007 <https://iopscience.iop.org/article/10.1088/1748-9326/10/9/094007>
25. Ridley, Jeff; Menary, Matthew; Kuhlbrodt, Till; Andrews, Martin; Andrews, Tim (2019). MOHC HadGEM3-GC31-MM model output prepared for CMIP6 CMIP. Version 20200515. Earth System Grid Federation. <https://doi.org/10.22033/ESGF/CMIP6.420>
26. Schaller, N., Kay, A.L., Lamb, R., Massey, N.R., van Oldenborgh, G.J., Otto, F.E.L., Sparrow, S.N., Vautard, R., Yiou, P., Ashpole, I., Bowery, A., Crooks, S.M., Haustein, K., Huntingford, C., Ingram, W.J., Jones, R.G., Legg, T., Miller, J., Skeggs, J., Wallom, D., Weisheimer, A., Wilson, S., Stott, P.A., Allen, M.R., 2016. Human influence on climate in the 2014 Southern England winter floods and their impacts. *Nat. Clim. Change*, 6 (6). <https://doi.org/10.1038/nclimate2927>
27. Sexton DMH, McSweeney CF, Rostron JW et al (2021) A perturbed parameter ensemble of HadGEM3-GC3.05 coupled model projections: part 1: selecting the parameter combinations. *Clim Dyn* <https://doi.org/10.1007/s00382-021-05709-9>
28. Turner, S., Barker, L.J., Hannaford, J., Muchan, K., Parry, S. and Sefton, C. (2021), The 2018/2019 drought in the UK: a hydrological appraisal. *Weather*, 76: 248-253. <https://doi.org/10.1002/wea.4003>
29. Vautard, R., Christidis, N., Ciavarella, A., Alvarez-Castro, M., Bellprat, O., Christiansen, B., Colfescu, I., Cowan, T., Doblas-Reyes, F., Eden, Jonathan., Hauser, M., Hegerl, G., Hempelmann, N., Klehmet, Katharina., Lott, F., Nangini, C., Orth, R., Radanovics, S., Seneviratne, S., Yiou, P., 2018. Evaluation of the HadGEM3-A simulations in view of detection and attribution of human influence on extreme events in Europe. *Climate Dynamics*. <https://doi.org/10.1007/s00382-018-4183-6>
30. Vrac, M., Vaittinada Ayar, P. and Yiou, P., 2013, Trends and variability of seasonal weather regimes. *Int. J. Climatol.*, 34: 472-480. <https://doi.org/10.1002/joc.3700>
31. Yamazaki K, Sexton DMH, Rostron JW et al (2021) A perturbed parameter ensemble of HadGEM3-GC3.05 coupled model projections: part 2: global performance and future changes. *Clim Dyn*. <https://doi.org/10.1007/s00382-020-05608-5>

32. Yoshimura, Hiromasa; Shindo, Eiki; Mizuta, Ryo; Ishii, Masayoshi; Obata, Atsushi; Adachi, Yukimasa (2019). MRI MRI-ESM2.0 model output prepared for CMIP6 CMIP. Version 20190603. Earth System Grid Federation. <https://doi.org/10.22033/ESGF/CMIP6.621>
33. Yukimoto, Seiji; Koshiro, Tsuyoshi; Kawai, Hideaki; Oshima, Naga; Yoshida, Kohei; Urakawa, Shogo; Tsujino, Hiroyuki; Deushi, Makoto; Tanaka, Taichu; Hosaka, Masahiro; Yoshimura, Hiromasa; Shindo, Eiki; Mizuta, Ryo; Ishii, Masayoshi; Obata, Atsushi; Adachi, Yukimasa (2019). MRI MRI-ESM2.0 model output prepared for CMIP6 CMIP. Version 20211010. Earth System Grid Federation. <https://doi.org/10.22033/ESGF/CMIP6.621>

## Figures

**Figure 1**

Seasonal daily frequencies of the 30 weather patterns over the UK in both the ERA5 reanalyses and the HadGEM3-A model ALL forcings runs between 1979-2010. The points making up the boxplot for each of the patterns represent the 15 individual ensemble members, where the shaded box covers the interquartile range, the whiskers are the min and max values, and the dots represent outliers.

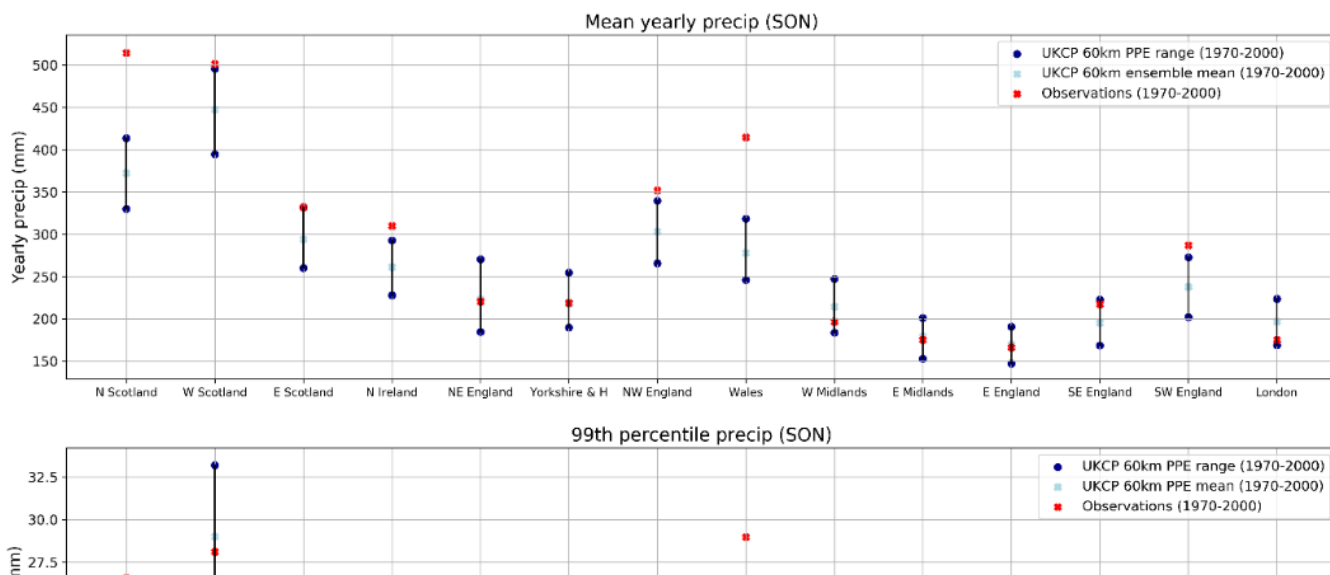


**Figure 2**

Validation of the UKCP Global (60km) 15 PPE for mean yearly and extreme daily rainfall (99<sup>th</sup> percentile) over the administrative regions of the UK when compared to the HadUK-gridded observations (red dots) between 1970-2000 in Autumn.

**Figure 3**

Seasonal frequencies of the 30 weather patterns over the UK of 15 ensemble members of HadGEM3-A ALL forcings runs (red) and NAT forcings runs (blue) from 1980-2010. The points making up the boxplots for each of the 30 patterns represent the frequency values for the 15 individual ensemble members, where the shaded box covers the interquartile range and the whiskers are the min and max values.

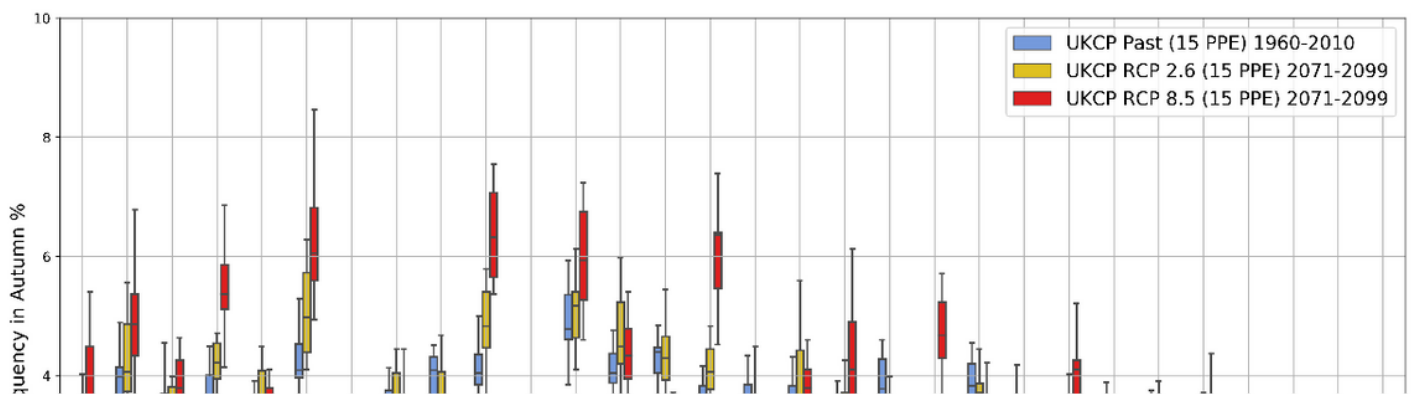


**Figure 4**

Plot showing Autumn seasonal frequencies of daily regime numbers for the 30 patterns for different time-slices and emissions scenarios using UKCP Global. The points making up the boxplots for each of the 30 patterns represent the frequency values for the 15 individual ensemble members, where the shaded box covers the interquartile range and the whiskers are the min and max values.

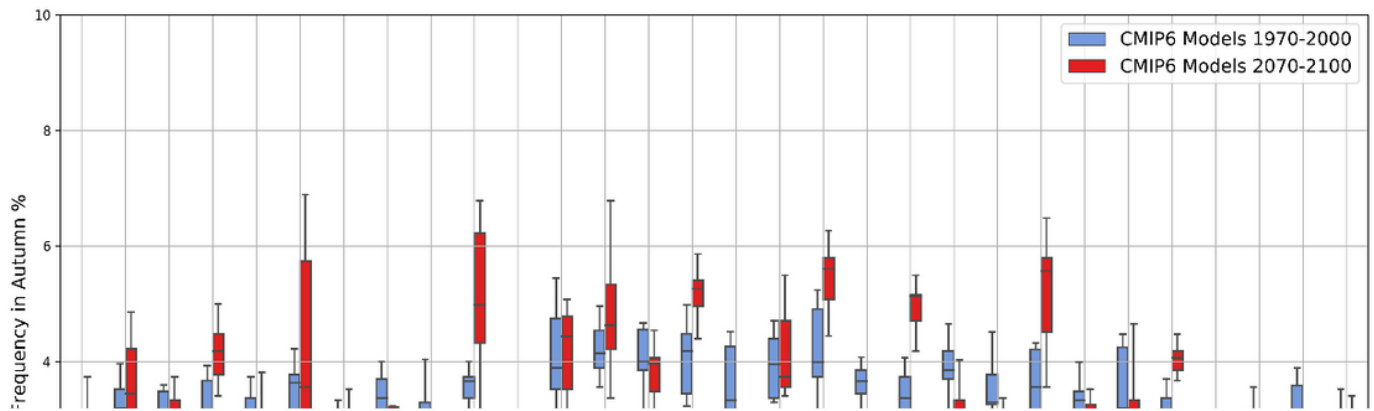


**Figure 5**

Plot showing Autumn seasonal frequencies of daily pattern numbers for the 30 weather patterns as boxplots for a past period (red) and a future period (blue) for the CMIP6 models used. The 9 points using CMIP6 models come from MRI-ESM2-0 ssp370 (5 ensemble members) and HadGEM3-GC31 MM ssp585 (4 ensemble members). The points making up the boxplots for each of the 30 patterns represent the frequency values for the 9 individual ensemble members, where the shaded box covers the interquartile range and the whiskers are the min and max values.

**Figure 6**

The transient evolution of daily weather pattern frequencies in SON for summer-types (Regimes 1-6) and winter-types (Regimes 25-30) between 1900-2100 in 10-year time-slices for the 15 Global UKCP PPE under emissions scenarios RCP 2.6 (dashed lines) and RCP 8.5. The shaded regions responding to summer and winter types represent the 10-year time-slice frequency ranges between 1900-2000.



**Figure 7**

The grid boxes used for the 3 Regions of the UK analysed for rainfall changes using the N216 grid for UKCP Global

## Supplementary Files

This is a list of supplementary files associated with this preprint. Click to download.

- [SupplementaryMaterialWeatherRegimesPaperCotterill.docx](#)